Atomic Energy of Canada Limited

THE OXIDATION, HYDRIDING AND AQUEOUS CORROSION OF U_3Si ALLOYS

by

M.A. FERADAY

Chalk River, Ontario

November 1971

AECL-3862

DISCLAIMER

THE OXIDATION, HYDRIDING AND AQUEOUS CORROSION OF U_3Si ALLOYS

by

M.A. Feraday
Fuel Materials Branch

SYNOPSIS

Specimens of U_3Si were heated in air and in hydrogen at temperatures up to 550°C and the products of reaction studied. The phases observed in these tests are compared with those which form in U_3Si samples corroded in high temperature water.

The aqueous corrosion of U_3Si is mainly an oxidation reaction although limited hydriding may also occur as a secondary reaction. The oxidation of U_3Si either in air or water appears to be a multi-step process in which most of the phases of the uranium-silicon system form. Due to the kinetics of formation and stability of the phases at various temperatures all are not observed in an individual test.

Although molecular hydrogen will not react with U_3Si directly, in some cases it will react with free uranium to form UH_3. If the UH_3 is subsequently oxidized, nascent hydrogen will be released which will react with the U_3Si.

Chalk River Nuclear Laboratories
Chalk River, Ontario
November, 1971

AECL-3862

Oxydation, hydruration et corrosion aqueuse des alliages de U_3Si

par

M.A. Feraday

Résumé

On a chauffé des échantillons de U_3Si, dans l'air et dans l'hydrogène, à des températures allant jusqu'à 550°C et on a étudié les produits de réaction. Les phases observées dans ces essais sont comparées à celles des échantillons de U_3Si corrodés dans l'eau à haute température.

La corrosion aqueuse de U_3Si est principalement une réaction d'oxydation bien qu'une hydruration limitée puisse également se produire sous forme de réaction secondaire. L'oxydation de U_3Si, dans l'air ou dans l'eau, semble être un processus à échelons divers où se forment la plupart des phases du système uranium-silicium. Par suite de la cinétique de formation et de la stabilité des phases, à différentes températures, il n'est pas possible de les observer toutes dans un simple essai.

Bien que l'hydrogène moléculaire ne réagisse pas directement avec l'U_3Si, il peut dans certains cas réagir avec de l'uranium libre pour former de l'UH_3. Si cet UH_3 est postérieurement oxydé, de l'hydrogène naissant sera libéré, lequel réagira avec l'U_3Si.

L'Energie Atomique du Canada, Limitée
Laboratoires Nucléaires de Chalk River
Chalk River, Ontario

INDEX

THE OXIDATION, HYDRIDING AND AQUEOUS CORROSION OF U_3Si ALLOYS

by

M.A. Feraday

1. INTRODUCTION

Uranium silicon alloys (containing about 4 wt% Si) are being developed for use in CANDU-type power reactors, fuelled with natural uranium and cooled by pressurized water or boiling water, because of expected reductions in unit energy costs (1). An important requirement for such fuel is that an element containing a defect hole in the sheath must operate for some time (possibly a few days), without undergoing unacceptable mechanical damage or release of uranium to the coolant system. This requirement arises from the economic importance of maintaining the reactor at power until the fuelling machine removes the defective element. Thus the behaviour of U_3Si when exposed to water/steam at fuel operating temperature is of importance to its application.

Post-irradiation metallographic examinations of fuel from U_3Si elements tested in-reactor with a defect hole in the Zircaloy sheath show that the reaction between U_3Si and water or steam is a highly complicated one in which several phases are formed (2). Development of possible methods of reducing the corrosion rates could be assisted by a knowledge of these reactions and the phases which are formed. Identification of the phases formed during the in-reactor tests by means of the electron probe microanalyser or by X-ray diffraction has not been possible because the equipment at CRNL cannot examine highly radioactive samples. The work reported here involved attempts to duplicate, in the laboratory, the structures observed in the irradiated samples. These inactive samples were then subjected to electron probe and X-ray diffraction analysis.

Possible reactions which could occur during an in-reactor defect test are:

1) oxidation of the U_3Si by water/steam with the release of nascent hydrogen, and
2) hydriding of the U_3Si.

An attempt has been made to determine the relative importance of each in the aqueous corrosion process. The experiments involved a determination of the effects of air, hydrogen and steam on some U_3Si samples containing residual U_3Si_2 particles and on others containing free uranium.

2. BACKGROUND

In the uranium-silicon alloy system, there is general agreement as to the existence, structure and general composition of the phases at either end of the phase diagram (Figure 1), i.e. U_3Si, U_3Si_2 and USi_3 (3,4,5,6).

In the 10-20 wt% Si region of the diagram some discrepancies exist as to the composition and lattice parameters of the phases (Table 1), e.g. three different crystal structures have been reported for the composition U-19 wt% Si (3,4,5). More experimental work is required to resolve these discrepancies. Although it is not certain which phases actually exist, in the following report it has been assumed that Zachariasen's (4) αUSi_2 and βUSi_2 (silicon deficient) are the phases occurring in the central region; Figure 1 shows the uranium-silicon phase diagram published by Kaufmann et al (3) and modified slightly to include Zachariasen's α and βUSi_2 (4).

Oxidation tests on U-Si alloys (9,10,11,12) have provided little evidence regarding identification of the phases which form or the reactions which occur. Although no deliberate hydriding tests have been done, several authors (on the basis of aqueous corrosion tests) found no evidence to show that U_3Si reacts with hydrogen (11,13,14,15), or that hydrogen will increase the aqueous corrosion rate of U_3Si (13).

3. EXPERIMENTAL

Table 2 shows the composition of the two uranium-silicon alloys (heats 458 and 466) which were studied in detail in the oxidation and hydriding tests. During preliminary trials, another alloy (heat 257) gave an interesting result so its composition is also included in Table 2.

Various batches of uranium-silicon alloys ranging in composition from 3.6 to 4.5 wt% Si were used in the aqueous corrosion tests. The spectrographic analyses of these alloys were similar to those of heats 458 and 466 in Table 2.

The alloys were supplied by Eldorado Nuclear Limited (Port Hope) in the form of cast rods which were heat-treated in vacuum for 3 days at 800°C to transform the as-cast structure of U_3Si_2 and uranium to U_3Si and some residual U_3Si_2 for alloys containing 3.8 to 4.5 wt% Si (Figure 2) or U_3Si with some residual uranium for alloys containing less than about 3.8 wt% Si (Figure 3). The rods were then machined to about 14.6 mm diameter to remove the cast surface. Solid rods for the oxidation and hydriding tests were cut into slugs about 13 mm long (30 grams), while hollow rods for the aqueous corrosion tests were cut into slugs ranging in length from 6 to 12 mm.

For phase identification, the specimens were mechanically polished down to 1/4 μm diamond using a Varsol lubricant, attack polished using ignited ammonium dichromate and 30% hydrogen peroxide for about two minutes, then etched in Murakami's reagent for various times. In some instances the samples were heat-treated in air at 120°C for 10 minutes to improve the contrast between the U_3Si and U_3Si_2 phases. The specimens were then examined on an optical microscope and on an electron microprobe analyzer.

The samples were oxidized in air at temperatures ranging from 350 to 550°C in a Lindberg box type furnace which permitted free access of air. Exposure times ranged from 45 minutes to about 28 hours. The samples were weighed before the test and after the loose oxide (which formed during the oxidation run) was brushed off. One sample was oxidized in oxygen and examined to see whether the reactions and corrosion products were the same as in air.

Hydriding of the U_3Si was done in a static atmosphere of hydrogen inside a quartz tube at pressures of about 10 and 100 Torr at temperatures from about 200 to 500°C. In each test, the tube was evacuated to 2×10^{-5} Torr before the hydrogen was added. The drop in hydrogen pressure and change in sample weight during each run were noted.

Environments for aqueous corrosion tests on U_3Si were either pressurized (86 bars) water at 300°C or atmospheric pressure steam at temperatures between 350 and 550°C. In the latter tests an argon atmosphere was used for the pre-heating period before the run and the cooling down period after the run; the temperature of the U_3Si pellet was recorded continuously in the steam tests. The details of the apparatus, the run conditions, and the corrosion rates have been (15a) or will be (15b) reported separately.

In addition to the unclad samples, a 50 mm long co-extruded specimen of heat-treated U-4 wt% Si clad in Zircaloy and containing a central void was tested. This sample, which was sealed at one end and open at the other to a supply of water, was heated in a furnace at 620°C for 4 hours to simulate the conditions inside an element at high temperature. A second specimen consisting of a slip-fitted cast U_3Si rod sealed inside a defected Zircaloy sheath was tested in 300°C water for 2340 hours.

4. RESULTS AND DISCUSSION

4.1 Reactions with Air and Oxygen

The results of the reactions of U_3Si alloys with air and oxygen at temperatures of 350, 450 and 550°C are summarized in Table 3.

In general, the results show that the samples formed a black coating which spalled off as a black powder (identified as U_3O_8, see below) during the test. Under this layer and adhering to the specimen was a thin black layer, a grey layer (in some cases) and a white layer adjacent to the U_3Si. Although the thin adherent black layer (identified as UO_2, Table 4) is present on all samples, the spalling showed that it is not protective. This UO_2 layer was approximately the same thickness in all tests.

X-ray analysis of the powder from sample No. 5 (oxidized 26.2 h at 350°C) and that from No. 6 (21.8 h at 350°C) showed

that U_3O_8 was present, but no UO_2 lines were observed in the diffraction pattern (19). Since SiO_2 has also been suggested as a product of the reaction of uranium silicides with air and water (11), it was looked for, but within the sensitivity of the analysis no SiO_2 was observed. Since the SiO_2 could be in an amorphous state, its presence may be difficult to detect. No trace of elemental silicon was observed in the diffraction pattern of either of these two powder samples (19).

Chemical analyses of the powder which spalled off several samples gave an average value of 15.2 wt% oxygen and 330 ppm nitrogen (Table 5). Fairly large variations (as high as ± 2 wt%) were observed in the oxygen analyses for duplicate samples indicating that the loose black powder may not be homogeneous. A silicon analysis on the powder sample from the sample oxidized in air gave a value of 3.2 wt% Si (Table 5); on sample dissolution in acid some of the residual particles were black, not white as for SiO_2, suggesting that at least some of the silicon was in some other form, possibly elemental silicon (16). If the corrosion product was only U_3O_8 and SiO_2 the theoretical oxygen value would be 17.7 wt%; the value would be 15.2 wt% if the products were U_3O_8 and Si and 14.7 wt% if UO_2 and SiO_2.

The results of the chemical analyses do not permit positive identification of phases but U_3O_8 was positively identified by X-ray diffraction. Other possible corrosion products could be SiO_2, Si, minor concentrations of UO_2 and/or ternary phases.

The low nitrogen analysis indicates that little nitriding occurred during the heating in air.

The adherent outer black layer observed on sample No. 5 (Figure 8) was identified by microprobe (Table 4) as UO_2. Adherent black layers observed on other uranium silicide alloys after oxidation and aqueous corrosion tests were identified as UO_2 by X-ray analysis (10,14). Identification of the grey layer is less certain. If it is assumed that oxygen makes up the difference in the probe analysis for sample No. 5 in Table 4, the composition of the grey layer would be U-3 wt% Si - 20 wt% O_2.

One ternary U-Si-O phase is $USiO_4$ (20) which has about the right oxygen content (19.4 wt%) but has a silicon content of 8.5 wt%. $USiO_4$ decomposes to UO_2 and amorphous silica (SiO_2) at temperatures between 400-500°C (20). Another phase recently identified (21) is $U_6Si_{11}O$; it has neither the silicon nor oxygen content of the grey layer.

The white layers were identified as either α or β USi_2 by microprobe examination (Table 4). A thin intermediate layer between the U_3Si and USi_2 in the sample (No. 12) heated in oxygen was identified at U_3Si_2.

4.2 Reactions with Hydrogen

The results of exposing U_3Si alloys to hydrogen at temperatures ranging from 200 to 500°C are summarized in Table 6.

In general, no change in weight or microstructure of the U_3Si pellets, nor any drop in hydrogen pressure was observed during the tests at 9.8 Torr at any temperature between 200°C and 500°C. This indicates that no significant amount of hydrogen was picked up by the samples regardless of whether they contained free uranium or free U_3Si_2. Similarly at 101 Torr and 225°C, no change in hydrogen pressure or in sample condition was noted during the test on sample No. 15 (free U_3Si_2).

In contrast, a small but significant decrease in hydrogen pressure was recorded during the 102 Torr, 225°C run with sample No. 14 (free uranium). Examination of this sample after the run showed that some of the uranium near the surface had transformed to a phase which appeared metallographically (22) like UH_3 (Figure 12) and has been assumed to be UH_3. No significant discoloration of the U_3Si around any of the uranium particles was observed. Subsequently, this sample was oxidized in air (120-150°C) and metallographic examination showed that the brown UH_3 particles had oxidized to UO_2 (Figure 13). The U_3Si around the oxidized uranium particles was darker than the U_3Si matrix after polishing and after polishing and etching (Figure 13), but not as dark as the UH_3 particles.

During the 127 Torr, 460°C run with specimen No. 20, a small pressure drop occurred during the run, but there was no significant change in sample weight. Some of the uranium particles touching the outer surface had been attacked but there was no darkening of the surrounding U_3Si.

No dimensional changes were observed in any of the deltized uranium silicide samples during hydriding runs.

Thus it appears that molecular hydrogen does not react with U_3Si or U_3Si_2 but does react with some of the free uranium particles in the alloy to form UH_3. Subsequently during the oxidation of the UH_3, the nascent hydrogen released diffuses into the adjacent U_3Si forming the darkened region which is thought to be either a ternary U-Si-H phase or a solution of hydrogen in the compound U_3Si. Analysis of this dark region on the electron probe has not been possible in these samples. Probe analysis of a similar dark region around corroded out uranium particles in an aqueous corrosion sample (section 4.3) indicates that there is no difference in either uranium or silicon composition between this area and the adjacent U_3Si (17), thus ruling out UH_3 and the $UH_{1.02}$ phase suggested by Burkart and Lustman (23). For convenience this darkened U_3Si will be called $U_3Si(H)$ in this report. There are no known ternary compounds of silicon, uranium and hydrogen.

It has been observed previously (24) that nascent hydrogen (e.g. produced by electrolysis) will enter in and move through metal much faster than molecular hydrogen. As an example, Barrer (24) has shown that the permeation of nascent hydrogen in palladium is equivalent to the rate that would be expected if the pressure of the molecular hydrogen was raised to 10,000 atmospheres at the surface of the metal.

In considering the movement of hydrogen through the U_3Si it appears that at the temperatures and pressures used in these tests, surface effects and lack of chemisorption (25) prevent molecular hydrogen from penetrating into U_3Si and U_3Si_2. Under certain conditions molecular hydrogen can be chemisorbed into the free uranium present. On the other hand, dissociated hydrogen (from the decomposed UH_3 particles) can penetrate into the U_3Si much more freely to form either a ternary phase or an interstitial solution.

Since the diffusion times in the hydriding tests were very short, i.e. about 18 minutes (section 3), it would appear (Figure 13) that the diffusion rate of hydrogen ions in U_3Si is fairly rapid.

4.3 Aqueous Corrosion of U-Si Alloys

It is not proposed to report all the aqueous corrosion tests done on U_3Si at CRNL; only those providing data relevant to the interpretation of the corrosion mechanism occurring in heat-treated binary U_3Si alloys are discussed in this report. A summary of the results of the metallographic and microprobe examination of the samples is reported in Table 7.

A layer of black oxide formed on the surface of samples tested at 350-550°C and eventually spalled off as a black powder; the thicknesses of the loose layer varied with time and temperature and was much thicker at 550°C (15a). Under this layer and adjacent to the U_3Si was a white layer or layers (U_3Si_2, USi_2 - see Table 7 and Figures 15, 18 and 19).

Chemical analysis (16) of the loose oxide from a sample corrosion tested in 550°C steam showed it to contain 16.1 wt% oxygen and 3.1 wt% silicon. This result suggests that the corrosion product in water is similar to that produced on samples oxidized in air (section 4.1) i.e. mainly U_3O_8.

The composition of the white layer appears to depend on the test temperature and the exposure time. At temperatures of 300-350°C and times of five hours or less, the layer formed was βUSi_2; during one longer run (115 hours) at these temperatures the layer formed was αUSi_2 (No. 28). During tests in the 450-550°C range, a thin layer of U_3Si_2 was formed along with the βUSi_2 layer. At 620°C the phases USi_3 and αUSi_2 were the only ones identified in the alloy from element No. 27.

Microprobe examination of the phase which is called βUSi_2 in this report shows compositions ranging from 14.6 to 16.0 wt% Si. In some cases this phase appeared laminated under polarized light (No. 26, Table 7) while in other cases it did not polarize (No. 22). No correlation of structure with silicon

concentration was found. The variation in silicon level could be due to the analytical tolerance of the probe or to the variation in silicon thought to exist in βUSi_2 (4).

In addition to the different structures observed in βUSi_2 under polarized light, this phase which is white in the as-polished condition may remain white (Figure 15) or turn darker (brown) (Figure 19) when etched in Murakami's reagent. Similarly αUSi_2 remained white after etching in one sample (No. 28) and turned darker (brown) in another (No. 27).

In general, U_3Si_2 particles did not appear to change in composition in advance of the corrosion front, since U_3Si_2 particles have been identified by the probe in the U_3Si matrix at the corrosion front (Figure 19), in the βUSi_2 (Figure 19) and in the αUSi_2 (Figure 22). However, in the latter higher temperature sample No. 27 several U_3Si_2 particles near the corrosion front had changed to a dark (tan colored) phase which appeared metallographically similar to the αUSi_2 nearby. In the same sample a white filament phase was observed in a U_3Si_2 particle (Figure 23) near the corrosion front where the white USi_3 was observed (Figure 20).

Probe analysis of the darkened areas around the U_3Si_2 particles and corroded uranium particles in sample No. 21 indicates that there is no significant difference in either uranium or silicon composition between these regions and the adjacent U_3Si (17). An electron microscopy examination of replicas (polished surface) of these darkened areas show that they have a rougher texture than that of the matrix U_3Si (26), however, no distinct phase boundaries were observed.

Since similar dark regions have been observed in the hydriding tests, it is believed that those observed in Figure 14 are formed by the reaction of corrosion product hydrogen with U_3Si. What is believed to be hydriding around U_3Si_2 particles (Figure 16) and at U_3Si grain boundaries (Figure 17) has been observed in other samples.

It is not fully understood why the U_3Si preferentially hydrides around U_3Si_2 and uranium particles and at grain boundaries. This reaction may be related to the surface energies

associated with the interphase and intergranular boundaries, or with a higher diffusion rate of hydrogen along the boundaries rather than in the U_3Si matrix.

5. SUMMARY

Examination of the aqueous corrosion results in light of the results in sections 4.1 and 4.2 suggests that two separate reactions, oxidation and hydriding, are occurring in the aqueous corrosion of U_3Si. Although oxidation is the most prominent reaction, limited hydriding of the U_3Si may occur as a secondary reaction. In the oxidation tests in addition to the outer uranium oxide layer, the U-Si phases $U3Si_2$, βUSi_2, and αUSi_2 were observed at various temperatures; in addition to these phases, USi_3 was noted in an aqueous corrosion test sample. Only one compound (USi) of those normally reported in the binary U-Si system has not been seen. Thus the oxidation of U_3Si is a complicated process with the formation of an outer oxide skin and an inner "pseudo" binary system where many of the phases in the U-Si system may form.

5.1 Oxidation Reaction

Consider now the initial reaction which occurs between the U_3Si and the oxygen (from the air or steam). The oxygen ions react with the uranium atoms at the U_3Si surface to form a thin adherent layer of UO_2. Although some of the silicon released by the oxidation of the uranium is left behind in the oxide corrosion product, some diffuses into the U_3Si. As the silicon atoms concentrate at the U_3Si/UO_2 interface, the total free energy of the system changes due to the changes in the entropy and the enthalpy of mixing and due to lattice strain. At some point, the concentration of silicon atoms in the interface region is such that the total free energy of the system can be minimized by a lattice and composition change from U_3Si to USi_x and from USi_x to USi_{x+1} etc.

During the next and subsequent steps in the oxidation process, the oxygen moves through the UO_2 layer to the USi_x/UO_2 interface where it reacts with the uranium in the USi_x phase. The excess silicon from this reaction then either results in the formation of the next U-Si phase which is kinetically favourable or diffuses into the USi_x phase (to the U_3Si/USi_x interface) to thicken up the USi_x layer. The thin adherent layer of UO_2 also oxidizes to form a thicker more friable layer of U_3O_8.

It is uncertain whether the oxygen moves through the thin adherent UO_2 layer by diffusion in the lattice or by mass movement through pores and microcracks. In either case the oxygen probably moves inwards through the UO_2 layer to the U-Si alloy/UO_2 interface rather than the U^{4+} ions or atoms diffusing out since it has been shown that the mobility of oxygen in UO_2 is much greater than that of uranium at all temperatures (27). Since the U_3O_8 does not form a coherent oxide and the porous cracked material offers little protection to the underlying oxide (UO_2), lattice diffusion need not be considered because rapid movement of oxygen would probably occur along the cracks in the U_3O_8.

A simplified schematic drawing of the possible stages of oxidation of U_3Si is shown in Figure 24; in this figure it has been assumed that only USi_2, UO_2 and U_3O_8 are formed as corrosion products of U_3Si, and that oxygen moves through the UO_2 layer by diffusion.

5.2 Transformations Within the U_3Si-USi_x System

Within the binary system, all phases present in the U-Si phase diagram should have formed since they are all thermodynamically stable. However as Kidson and Miller point out (28) although the equilibrium diagram indicates that all phases will form in a diffusion zone, the kinetics of nucleation and growth of certain phases may be so slow that these phases will not form in detectable amounts during short periods.

Some of the reasons why certain U-Si phases form preferentially while others are not observed may be attributed to the following factors. A phase region may be vanishingly thin i.e. it is present but not observable under normal procedures. Alternately if the process is not a simple bulk diffusion controlled reaction the nucleation of the new phase may be the controlling step.

A study of layer growth during interdiffusion in the Ni-Al system showed that while four phases occur in the equilibrium diagram, all of these were not observable in the diffusion couples under all time and temperature conditions (29). From these results Castleman and Seigle concluded that the growth of all four phases in the Ni-Al system is controlled by volume diffusion. In similar studies on the Al-Zr system Kidson and Miller, (28) observed only one of the nine phases which occur on the phase diagram. They concluded that the formation of this compound ($ZrAl_3$) in preference to others could be explained in terms of the phase structure.

Assuming that a phase does form, Kidson and Miller (28) give the following expression for the width of any phase β as a function of time (t) and temperature (T):

$$W_\beta(T,t) = \left[A_{\beta\gamma}(T) - A_{\alpha\beta}(T)\right] t^{\frac{1}{2}}$$

where $A_{\beta\gamma}(T)$ and $A_{\alpha\beta}(T)$ are rate constants which are independent of time but depend on the diffusion coefficients, the miscibility gap and the solubility range. An increase in time should cause all phases to thicken but it should not affect the rates of growth. In general it is assumed that a process is governed by volume diffusion if a parabolic relationship is observed between the width of the diffusion zone and the annealing time. A departure from this parabolic behaviour indicates that some other effect (e.g. rate of nucleation of new phases, the presence of an oxide film) which was not considered in the simple diffusion case is in operation. Also since both of the 'A' terms have a complicated temperature dependence, the width of a phase will not vary with temperature in a simple Arrhenius manner.

In the qualitative results reported here the U-Si system is reasonably well behaved since most of the phases were observed. Although thickening up of some of the phase layers with time is known to occur (Samples 3,4,8 and 10) there are not enough results to test for parabolic growth rate dependence.

The temperature dependence of the formation and growth of the phases is as follows:

a) USi_3 - only observed after the 620°C test. This result suggests that factors other than those considered in the simple diffusion model may be operative

b) αUSi_2 - present after short term tests at 450, 550 and 620°C. This phase was also present in one longer test (#28) at 295°C which suggests that an incubation period may exist for the formation of this phase at lower temperatures; this is not allowed for in Kidson's simple treatment

c) βUSi_2 - this is normally the phase that was observed in the range 300-350°C, but it was also observed at 450 and 550°C

d) U_3Si_2 - only observed as a thin layer in two tests (#12&#25) at 550°C. This result is inconsistent with Kidson's simple diffusion model.

Some of the inconsistencies in phase formation may also be explained by the non-ideal conditions which existed in the tests. The test temperatures reported are those of the furnace and do not take into consideration the rise in temperature which is thought to have occurred in some samples due to the exothermic heat of reaction. Other factors such as oxide buildup, surface cracks and slow nucleation rates may also limit phase formation even in ideal isothermal conditions.

Thus while Kidson's simple diffusion model is useful in analyzing the results, it appears that effects which were neglected in the simple model are operative in the complicated U-Si system. The concepts employed by Kidson and Miller (28) and Castleman and Seigle (29) could be used in a more detailed study of the time and temperature dependence of phase formation in the U-Si system to determine the rate controlling processes in the oxidation of U_3Si.

5.3 Hydriding

U_3Si containing only excess U_3Si_2 is not hydrided by molecular hydrogen at temperatures up to 500°C and pressures up to 120 Torr. Under certain conditions, molecular hydrogen will react with some of the free uranium present in U3Si to form UH_3. Subsequent exposure to air at temperatures as low as 120°C will oxidize the UH_3 and release nascent hydrogen, which may react with the surrounding U_3Si to form a new phase or an interstitial solution. The affected region is darker in color than the surrounding U3Si and has uranium and silicon levels which are comparable to those of U_3Si.

During aqueous corrosion of U_3Si, nascent hydrogen from the corrosion reaction is available to react with U_3Si. Such reactions have been observed around U_3Si_2 and uranium particles, and at grain boundaries.

6. REFERENCES

1. G.H. Chalder, W.T. Bourns, M.A. Feraday and J. Veeder, "U_3Si as a Nuclear Fuel", AECL-2874 (May, 1967).

2. M.A. Feraday, G.M. Allison, J.F.R. Ambler, G.H. Chalder and J.J. Lipsett, "In-Reactor Performance of Defected Zircaloy Clad U_3Si Fuel Elements in Pressurized and Boiling Water Coolants", AECL-3106 (May, 1968).

3. A. Kaufmann, B. Cullity and G. Bitsianes, "Uranium Silicon Alloys", Trans. AIME 209, 23, January 1957.

4. W.H. Zachariasen, "Crystal Chemical Studies of the 5f Series of Elements", Acta Cryst. 2, 94, 1949.

5. A. Brown and J.J. Norreys

   a) "Beta Polymorphs of Uranium and Thorium Disilicides", Nature 183, 673 (1959).

   b) "Uranium Disilicide", Nature 191, 61 (1961).

6. P. Gross, C. Hayman and H. Clayton, "Heats of Formation of Uranium Silicides and Nitrides", Thermodynamics of Nuclear Materials IAEA (Vienna) 1962, p.653.

7. U.G. Brauer and H. Haag

   a) "Notiz uber die Kristallstruktur von Uransilicid", Zeit. fur Anorg. Chemie 259, 197, (1949).

   b) "Uber Darstallung und Kristallstruktur der Disilicid ..", Zeit. fur Anorg. Chemie 267, 198 (1952).

8. A.S. Berezhnoi, "Silicon and its Binary Systems", Consultants Bureau, New York (1960), U-Si phase diagram corrected according to Zachariasen (4).

9. W.D. Wilkinson, "Uranium Metallurgy", Vol. 2, Interscience Publishers (1962).

10. W.M. Albrecht and B.G. Koehl, "Reactivity of Uranium Compounds in Several Gaseous Media", 2nd U.N. International Conference on Peaceful Uses of Atomic Energy, Geneva (1958) p.710.

11. L.O. Lock, G.B. Engle, M.J. Snyder and W.H. Ducksworth, "Survey of Refractory Uranium Compounds", BMI-1124 (1956)

12. M. Bloomfield, R.B. Gordon, B. Hayward and D.I. Sinizer, "U_3Si_2 Fuel Evaluation - Oxidation Characteristics", NAA-SR-Memo-5199 (20 April, 1960).

13. R.A. Wolfe, W.E. Bond, W.A. Bostrom, I. Cohen and R.B. Roof, Jr., "Development of U_3Si Epsilon Phase", WAPD-155 (1956).

14. S. Isserow, "The Uranium Silicon Epsilon Phase, NMI-1145 (1956).

15. W.T. Bourns,

a) "Corrosion Testing of Uranium Silicide Fuel Elements", AECL-2718 (1968).

b) Unpublished work at CRNL.

16. Analyses done by P. Hardy, D. Edwards, T.H. Longhurst, D. Bellevance and G.J. Jarbo of General Chemistry Branch at CRNL.

17. (Mrs.) T. Bethune, internal memoranda at CRNL to M.A. Feraday, November 12 and 26, 1969.

18. R.W. Gilbert - internal memorandum at CRNL to J.L. Conversi, 26 August, 1970.

19. (Miss) S.D. Collins, personal communication at CRNL (December 1969).

20. H.R. Hoekstra and L.H. Fuchs, "$USiO_4$", Science 123, 105 (1956).

21. P.L. Blum, J. Laugier, J-P Morlevat and H. Vaugoyeau, "On the Nature of the Hexagonal Silicide USi_2 and the Existence of a New Ternary Composition $U_6Si_{11}O$". C.R. Acad. Sc. Paris 262, 1856-1859 Series C (27 June 1966).

22. W. Evans, "The Metallography of Reactive Metals", Trans. Cdn. Mining & Met. Bulletin LXIII, 617-624 (1960) (Also as AECL-1148).

23. M.W. Burkart and B. Lustman, "Corrosion Mechanisms of Uranium Based Alloys in High Temperature Water", Trans. AIME 212, 26 (1958).

24. F.N. Rhines, "Gas-Metal Diffusion in Atom Movements", ASM Publication (1951).

25. G.G. Libowitz, "The Solid State Chemistry of Binary Metal Hydrides", W.A. Benjamin Co. Inc. (1965).

26. D.H. Rose, Internal memorandum at CRNL to M.A. Feraday, 7 October, 1970.

27. J. Belle, "Uranium Dioxide - Properties and Nuclear Applications", USAEC Publication (1961), pp 308 & 318.

28. G.V. Kidson and G.D. Miller, "A Study of the Interdiffusion of Aluminum and Zirconium", J. Nuc. Mater., 1959, 12, #1, 61-69 (1964).

29. L.S. Castleman and L.L. Seigle

a) Formation of Intermetallic Layers in Diffusion Couples" Trans AIME 209, 1173-74 (1957)

b) "Layer Growth during Interdiffusion in the Aluminum-Nickel Alloy System", Trans AIME 212, 589-96 (1958).

7. ACKNOWLEDGEMENTS

The author would like to acknowledge the helpful assistance of C. Grolway, J.L. Conversi and R.M. Condie in doing the oxidation and hydriding runs and discussions with J.R. MacEwan, G.H. Chalder and Professor H.W. Kerr (University of Waterloo).

The author would also like to thank the staff of the Metallurgical Engineering Branch for providing the L-series of photographs.

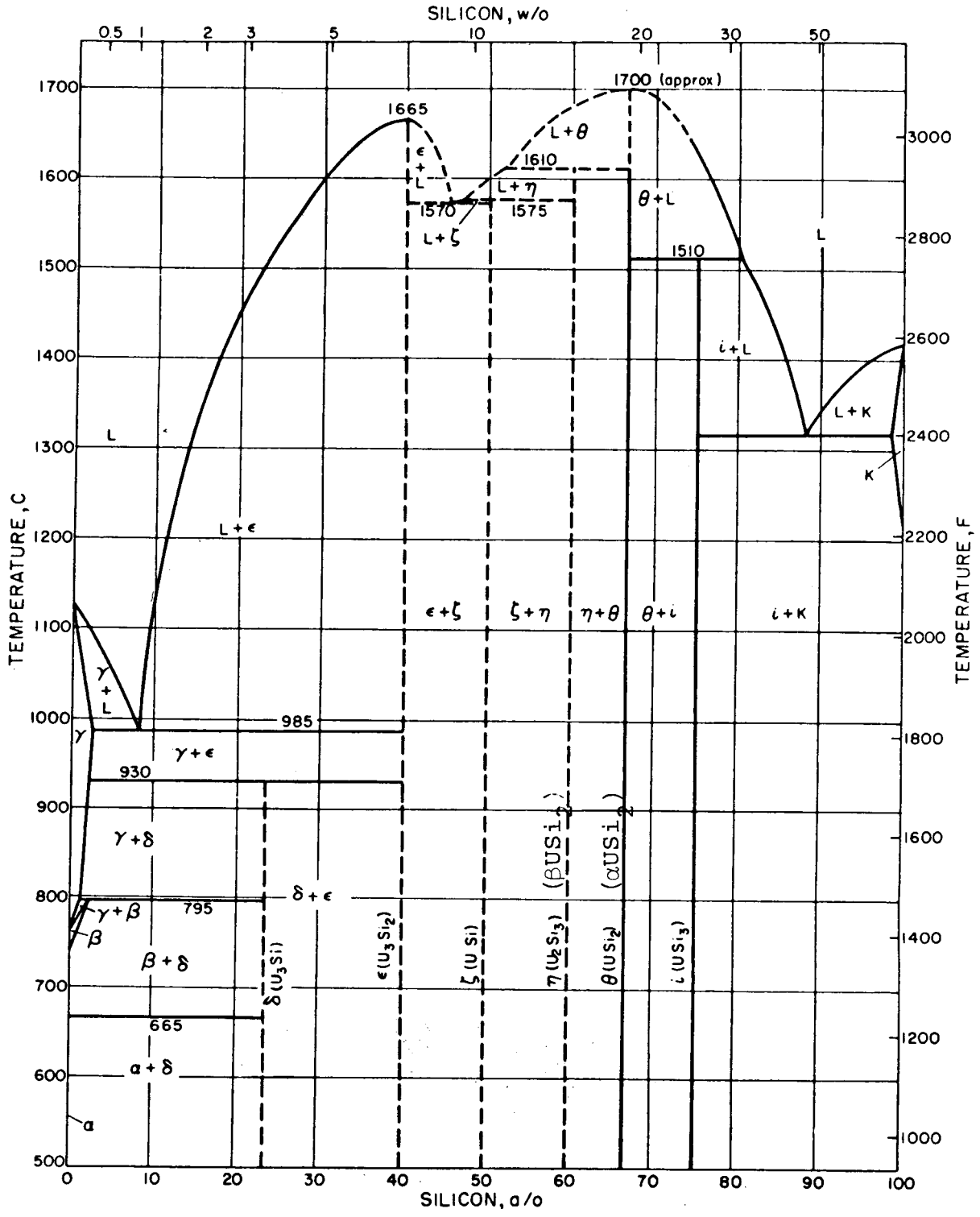

FIGURE 1

Uranium-Silicon Phase Diagram

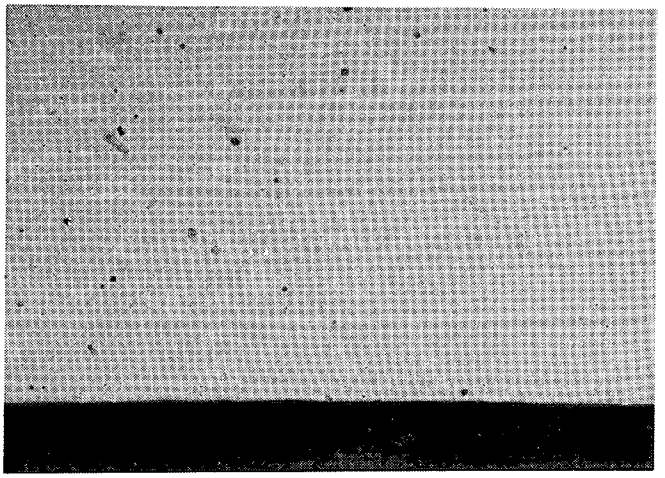

FIGURE 2

Heat 466 (4 wt% Si)

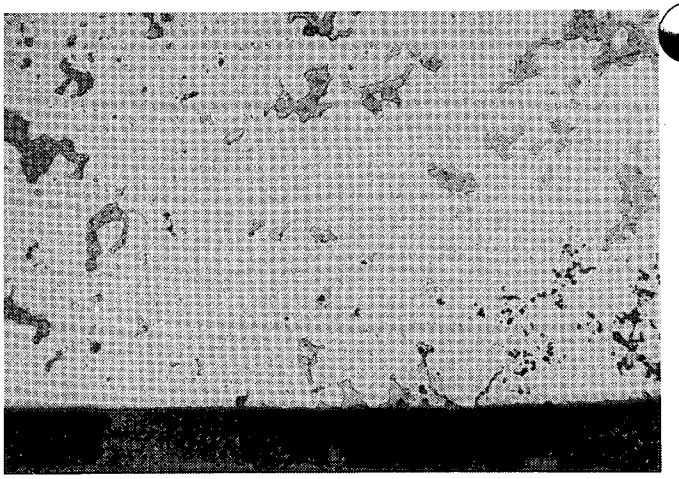

FIGURE 3

Heat 458 (3.45 wt% Si)

X200 (ETCHED) TYPICAL STRUCTURE OF THE HEATS USED IN THE OXIDATION AND HYDRIDING TESTS - SHOWING CLEAN OUTER EDGE AFTER MACHINING

Grey matrix - U_3Si
White particles - U_3Si_2

Dark grey particles - Uranium
Black spots - UO_2 + Porosity

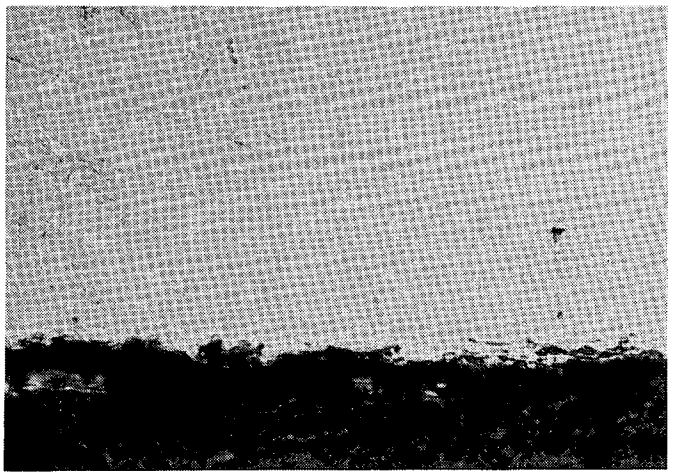

FIGURE 4 (X200) Etched

Layer of white phase on sample No. 4. (350°C - 25.5 h in air)*

* A thin layer of UO_2 was observed outside of the white layer but it is not shown in these figures.

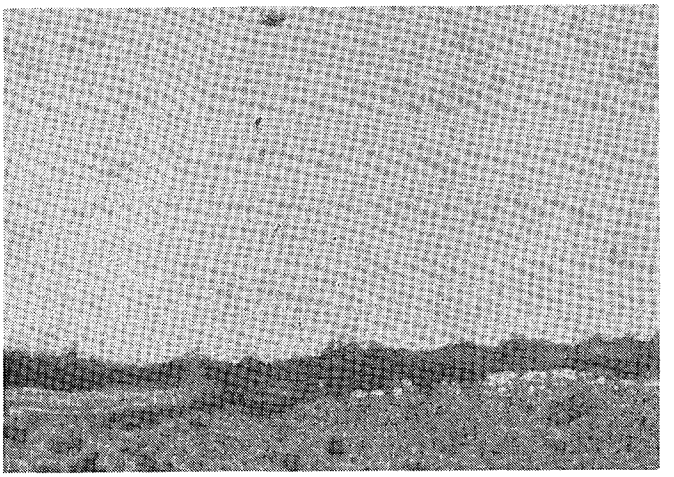

FIGURE 5 (X200) Etched

Layer of white phase on sample No. 3. Note that the free uranium (dark grey) protrudes through the white layer to the surface (350°C - 25.5 h in air).*

FIGURE 6 MACROPHOTOS OF THE SPECIMENS OXIDIZED IN AIR

Pellet and Oxide	Brushed Pellet	Pellet and Oxide	Brushed Pellet
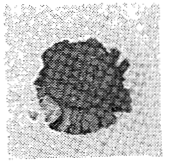		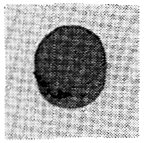	
Sample No. 4 350°C - 25.5 hours		Sample No. 3 350°C - 25.5 hours	
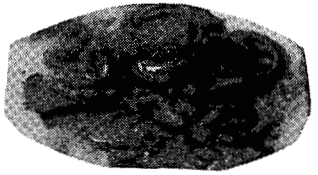	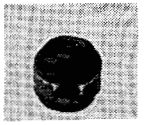	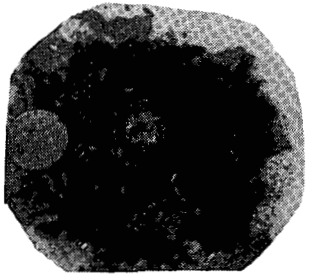	
Sample No. 8 450°C - 53 min.	Sample No. 8 450°C - 53 min.	Sample No. 7 450°C - 53 min.	Sample No. 7 450°C - 53 min.
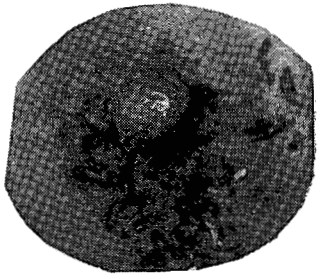	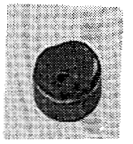	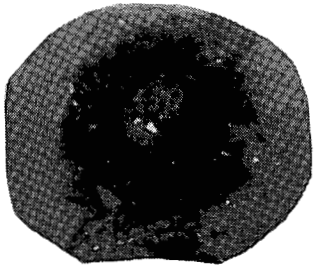	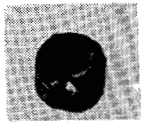
Sample No. 10 550°C - 48 min.	Sample No. 10 550°C - 48 min.	Sample No. 9 550°C - 48 min.	Sample No. 9 550°C - 48 min.

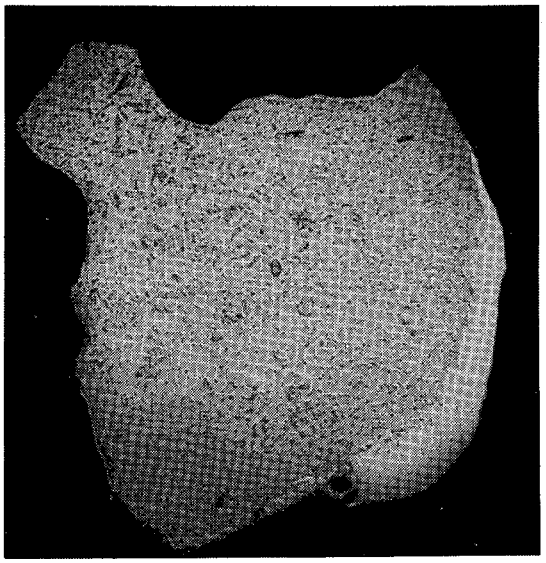

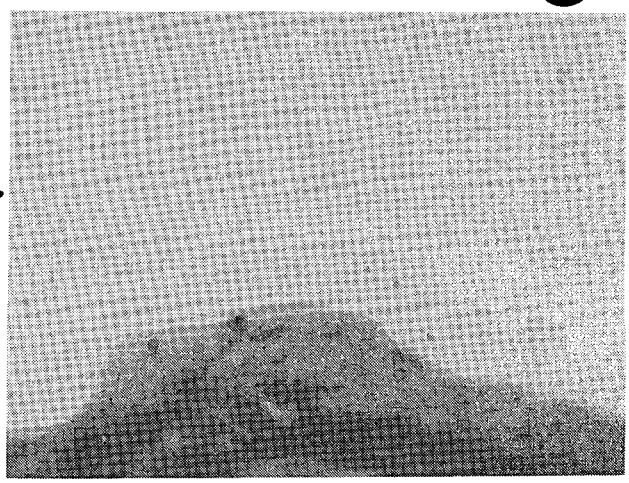

FIGURE 7 (X7.5)

Massive white layer is βUSi_2*

FIGURE 8 (X200)

SAMPLE NO. 5 SHOWING PHASES PRODUCED AFTER 26.2 HOURS IN 350°C AIR (ETCHED)

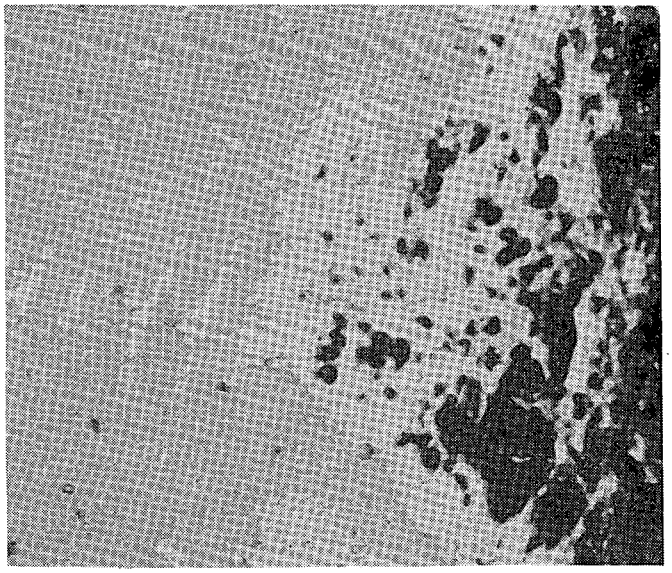

FIGURE 9 (X200) Etched

Typical porous white phase (βUSi_2)* on samples No. 6 and 10.

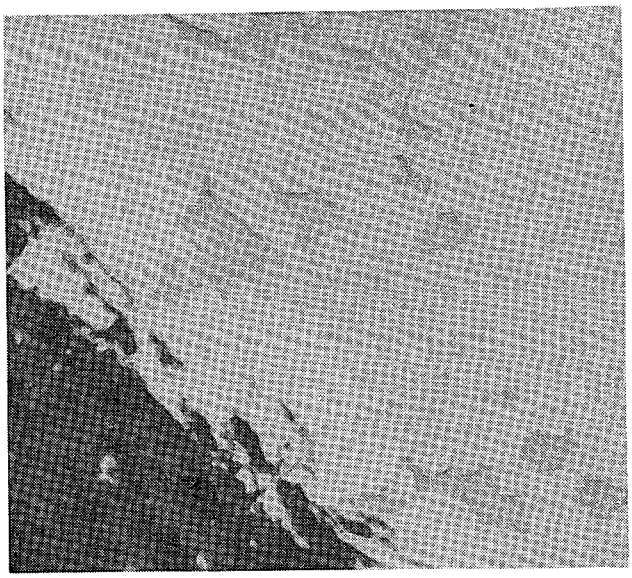

FIGURE 10 (X500) Etched

Sample No. 7 showing uncorroded uranium (dark grey) in the white layer.

* identified by microprobe (Table 4)

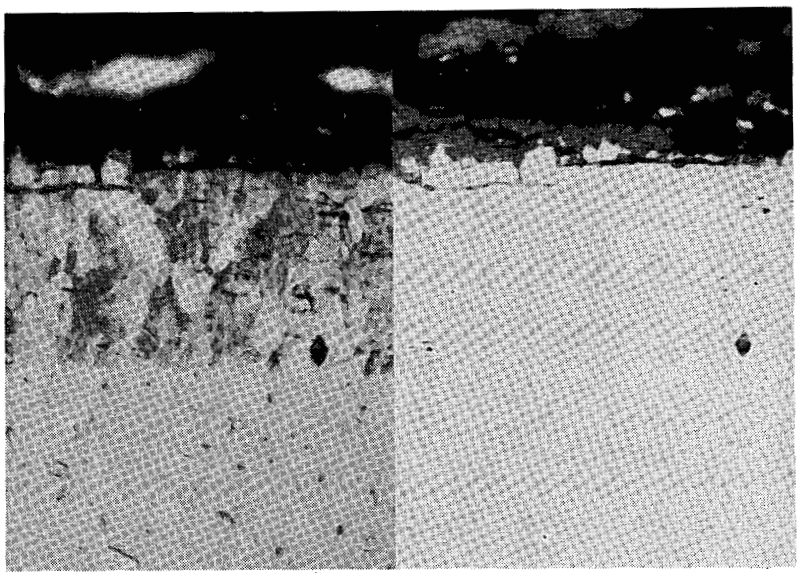

Polarized Bright Field

FIGURE 11 (X500)
As polished

Sample No. 11 showing white layer which had a laminated structure under polarized light. (α-USi_2)*

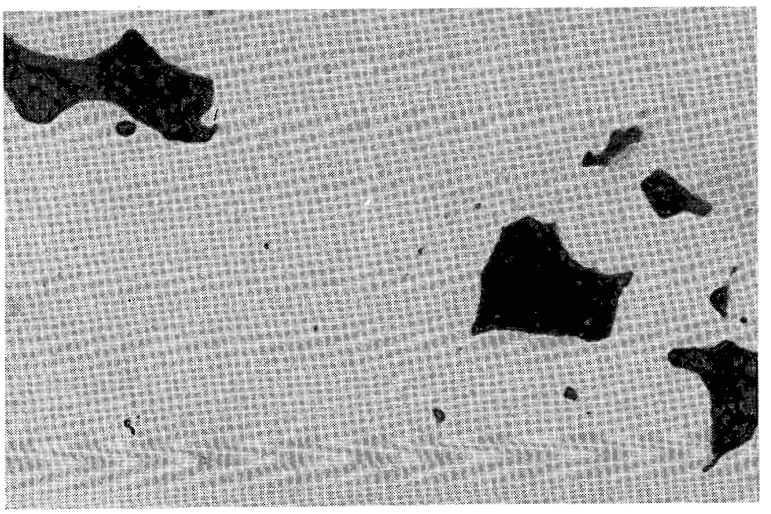

FIGURE 12 (X1000)
As polished

Sample No. 14 showing free uranium particles (light) and medium brown UH_3 particles (dark grey) in the U_3Si matrix.

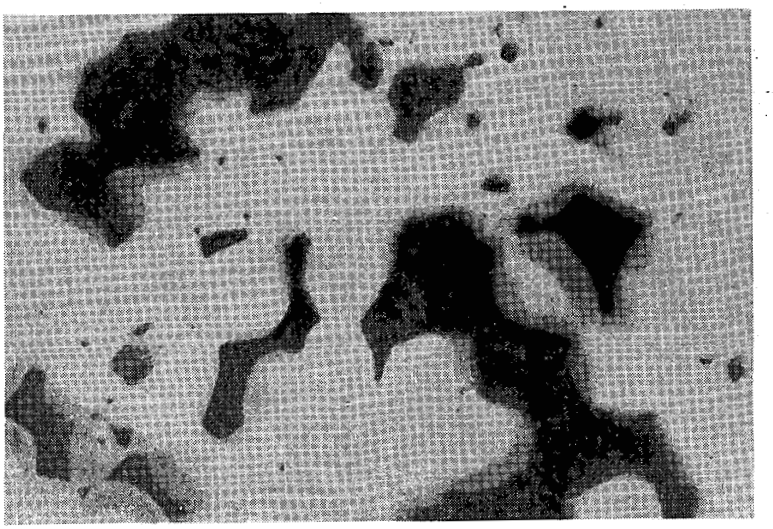

FIGURE 13 (X1000)
Etched

Sample No. 14 showing uranium oxide (black) formed from uranium particles. A darkening of the U_3Si matrix around these particles is seen.

* identified by microprobe (Table 4)

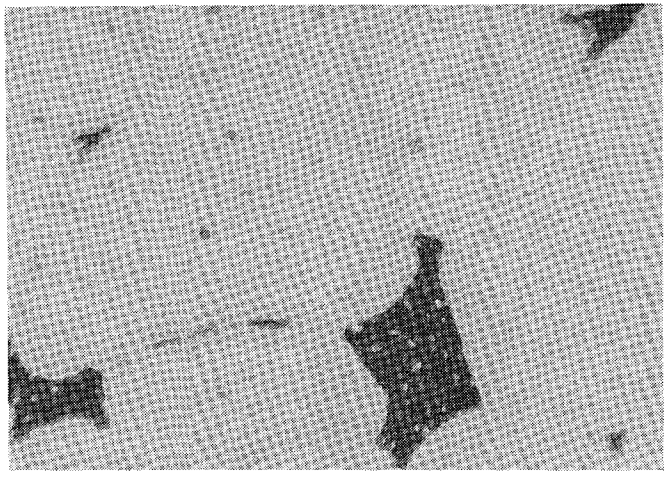

FIGURE 14

X1000
(etched)

Sample No.21 (320°C water) showing darkening of U_3Si* matrix around U_3Si_2* particles (white) and corroded uranium* particles (black).

FIGURE 15

X500
(etched)

Sample No. 23 (450°C steam) showing white layer (βUSi_2)* on surface. White particles in U_3Si matrix are U_3Si_2*. L-239-D4

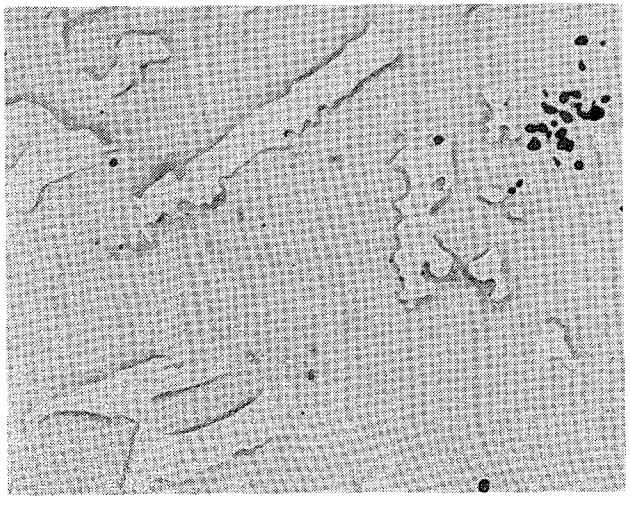

FIGURE 16 (X500) Etched (L-239-D1)

Sample No. 23 showing darkening of U_3Si around U_3Si_2* particles.

* identified by microprobe (Table 7)

FIGURE 17 (X500) Etched (L-227-B2)

Sample No. 24 (510°C) showing what is thought to be hydriding at U_3Si grain boundaries and around U_3Si_2 particles.

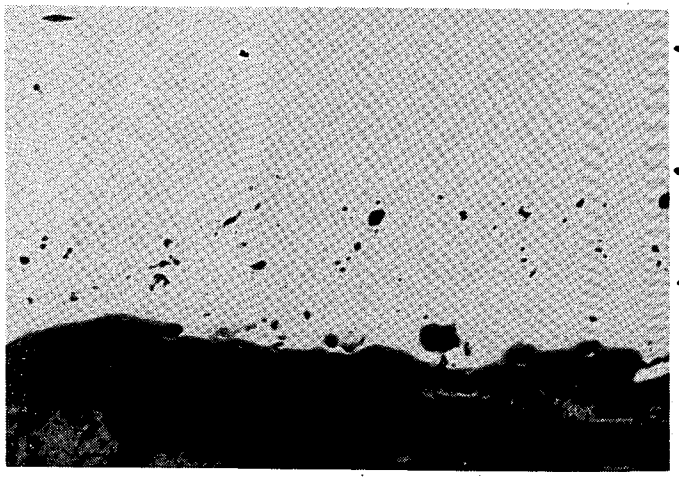

U_3Si^* with $U_3Si_2^*$ particles

$U_3Si_2^*$

β USi_2^* with $U_3Si_2^*$ particles

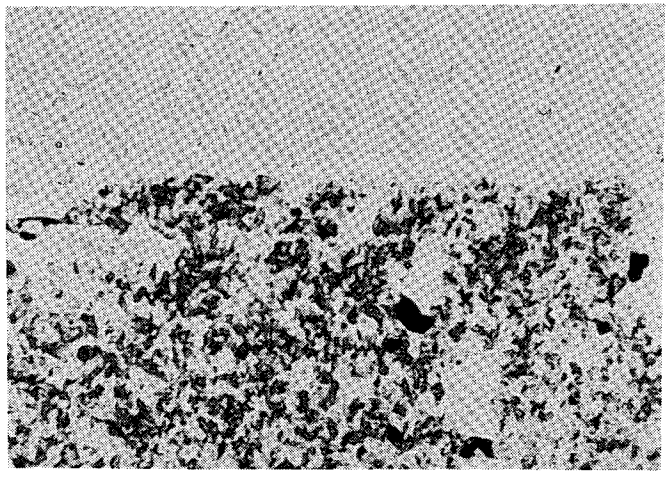

FIGURE 18 (X100) As polished L-227-A1

FIGURE 19 (X500) Etched L-227-A3

Sample No. 25 (550°C steam) showing thick layer of β USi_2 and thin layer of U_3Si_2. White β USi_2 layer (Figure 18) darkened when etched with Murakami's reagent (Figure 19).

* identified by microprobe (Table 7)

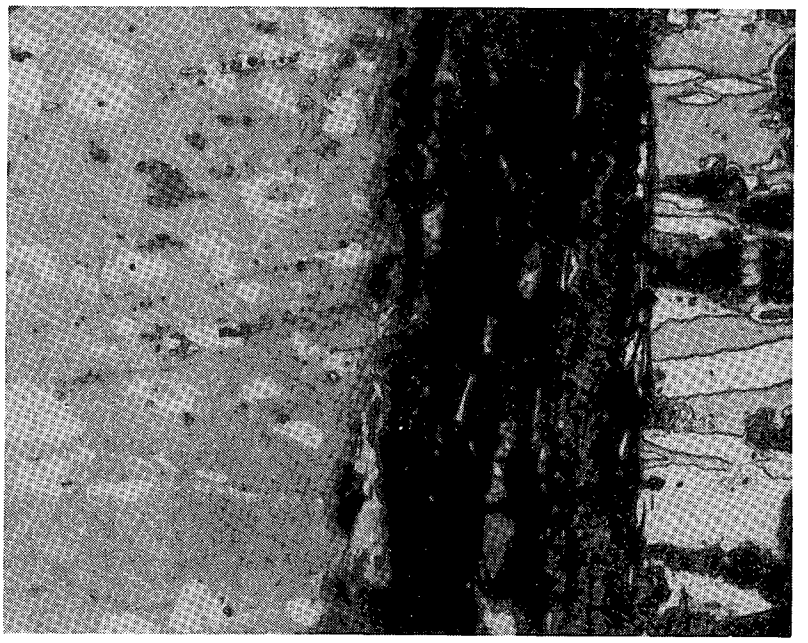

FIGURE 20 X250 (etched)

Sample No.27 showing islands of USi_3* (white) and α USi_2* (grey) in the black corrosion product. On the left is the main U_3Si (grey) with residual U_3Si_2 particles (white).

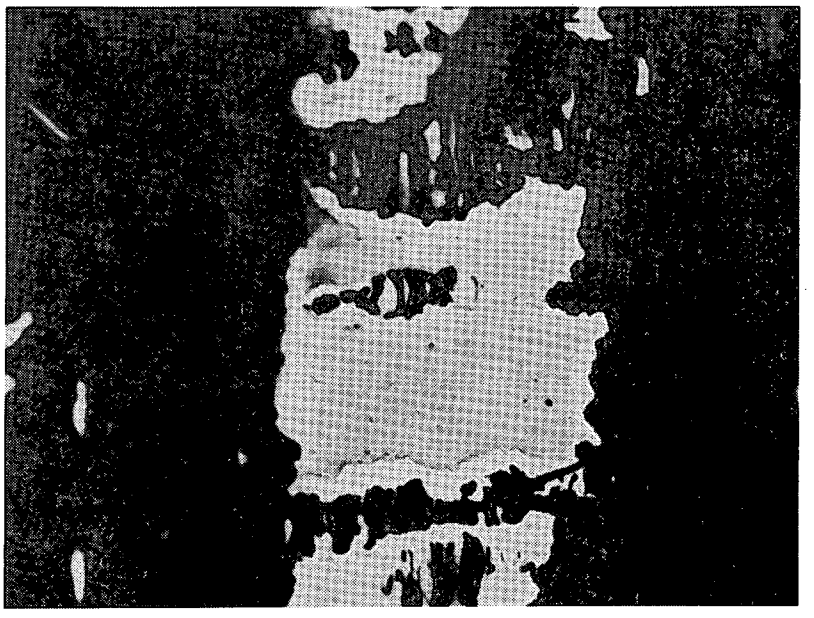

FIGURE 21 X500 (etched)

Sample No.27 showing islands of α USi_2* surrounded by a rim of USi_3* (white) in the black corrosion product.

* identified by microprobe - see table 7.

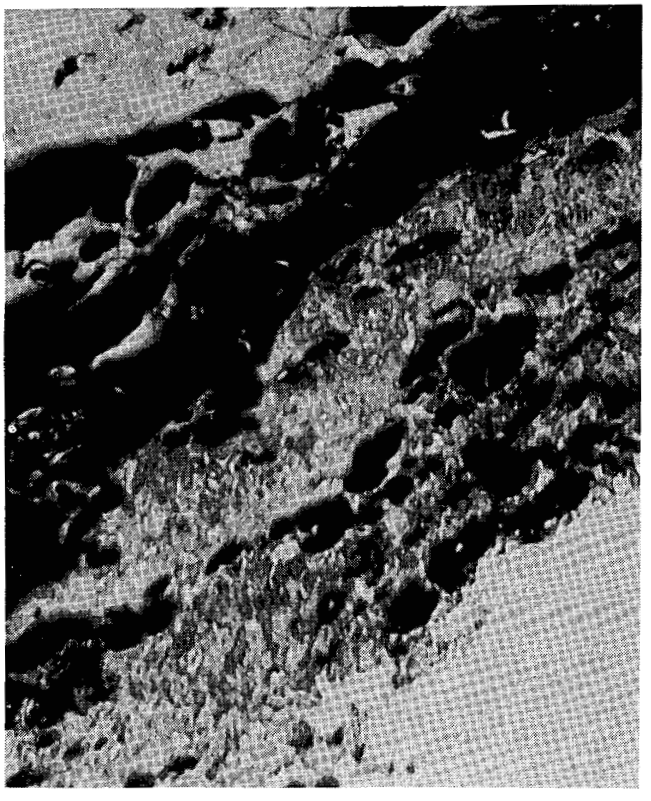

FIGURE 22 X250 (etched)

Sample 27 showing the αUSi_2 in the central void

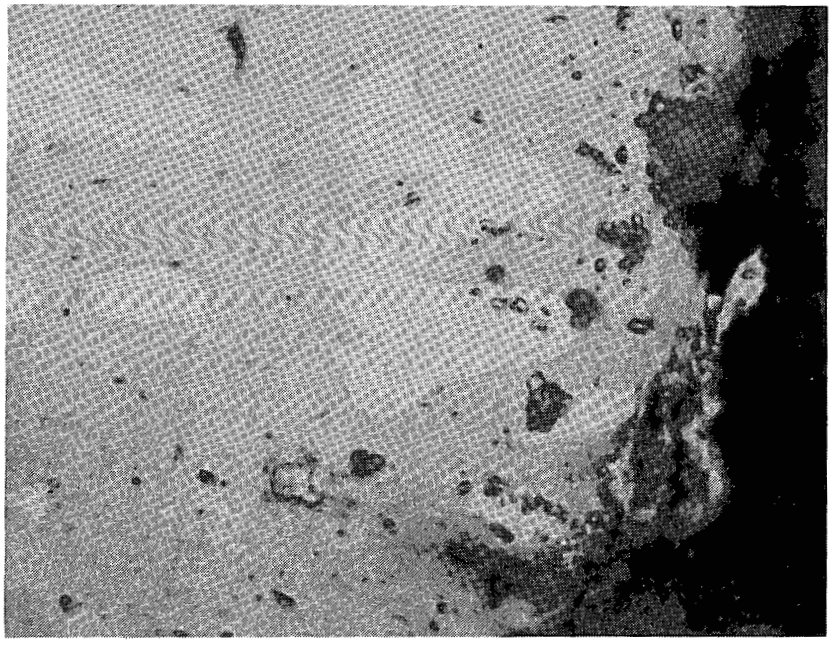

FIGURE 23 X1000 (etched)

Showing a white filament phase in a U_3Si_2 particle near the corrosion front. The matrix is U_3Si.

* identified by microprobe - see table 7.

FIGURE 24 DIFFERENT STAGES IN THE OXIDATION OF U_3Si

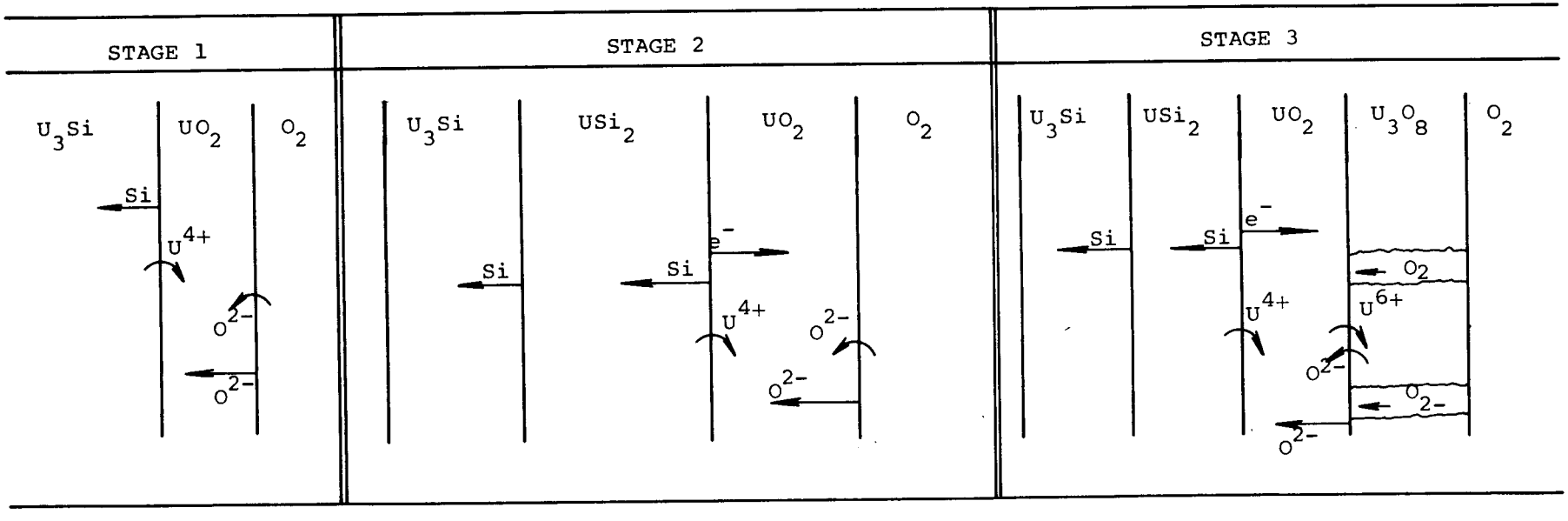

e^- = electron

TABLE 1

DATA ON PHASES IDENTIFIED IN THE U-Si ALLOY SYSTEM

Phase		Structure	Silicon (wt%)	X-ray Density (g/cm^3)	Lattice Parameters (Å)	Reference
U_3Si		B.c.t.	3.8	15.58	a = 6.020 ± 0.002 c = 8.696 ± 0.003	3,4
U_3Si_2		Tetragonal	7.3	12.20	a = 7.3298 ± 0.0004 c = 3.9003 ± 0.0005	3,4
USi	**	Orthorhombic	10.5	10.40	a = 5.66 ± 0.01 b = 7.66 ± 0.01 c = 3.91 ± 0.01	3,4
$USi_2(\alpha)$	**	B.c.t.	19	8.98	a = 3.98 ± 0.03 b = 13.74 ± 0.08	3,4
U_3Si_5	**	Hexagonal	16.4	NR	a = 3.843 ± 0.001 c = 4.069 ± 0.001	5,6
$USi_{1.88}$	**	Tetragonal	17.9	NR	a = 3.948 ± 0.002 c = 13.67 ± 0.001	5
USi_2	**	Hexagonal	19.1	NR	a = 4.028 ± 0.001 c = 3.852 ± 0.001	5
$USi_2(\beta)$*	**	Hexagonal	15-19	9.25	a = 3.86 ± 0.01 c = 4.07 ± 0.01	3,4,8
USi_2	**	Cubic	NR	7.8	a = 4.053	7
USi_3		Cubic	26.1	8.15	a = 4.0353	4

* also identified as U_2Si_3

** phases in the region of the phase diagram where uncertainties exist

NR Not recorded

TABLE 2

CHEMICAL AND SPECTROGRAPHIC ANALYSIS* OF U_3Si USED IN THE OXIDATION AND HYDRIDING STUDIES

1. Chemical Analysis

	Heat 458	Heat 466	Heat 257
Silicon (wt%)	3.45	4.03	3.61
Carbon (ppm)	65	60	80

2. Spectrographic Analysis in ppm

	Heats 458 and 466	Heat 257		Heats 458 and 466	Heat 257
Al	50	1200	Mn	4	-
B	0.5	-	Mo	<2	-
Bi	<5	-	Nb	<10	-
Ca	<10	-	Ni	110	130
Cd	0.3	-	Sn	10	-
Cr	25	-	Ti	<5	-
Cu	10	-	V	≈10	-
Fe	≈100	-	Zn	<10	100
Mg	<5	-	Zr	>100	1200

* done at CRNL[16].

TABLE 3 SUMMARY OF RESULTS OF AIR OXIDATION OF U_3Si SAMPLES (14.6 mm dia. x 13 mm long)

Sample No.	CRNL Reference No.	Temp. (°C)	Time	Weight of Sample (g)		Avg. thickness White layer (μm)	Remarks
				Before test	After test (brushed)		
1	458-1-4	350	1 h	33.8	33.7	Nil	Thin adherent oxide film*. No white or grey layer observed.
2	466-1-4	350	1 h	30.4	30.3	8	Thin adherent oxide film. Thin white layer observed.
3	458-2-2	350	4 + 21.5 h	31.6	30.4	20	After 4 hrs. - a tight adherent oxide* and a thin layer (10 μm max.) of white phase over 5% of surface. After 25.5 hrs. - small quantity of oxide spalled off (see Fig. 6). Adherent oxide layer under loose oxide. Continuous layer of white phase except in No. 3 where free uranium broke the surface (Figs. 4 & 5). Samples completely oxidized after a total of 28.2 hrs.
4	466-2-2	350	4 + 21.5 h	30.2	28.4	15	
5	458-2-5	350	26.2 h	32.4	17.9	See Figs. 7,8	Massive white layer (Fig. 7) did not polarize. When the thin white layer (Fig. 8) was viewed under polarized light it showed a laminated structure similar to Fig. 11. A grey layer observed adjacent to white phase (Fig. 8).
6	466-2-5	350	21.8 h	29.9	11.3	See Fig. 9	Porous white layer varying from 50 μm to 300 μm (Fig. 9). Small amount of grey phase in a crack.
7	458-2-3	450	25 + 28 m	31.7	28.9	70	After 53 min. sample badly corroded (Fig. 6). Uncorroded uranium seen in a dense white layer (Fig. 10). When viewed under polarized light this white layer showed a laminated structure similar to Fig. 11.
8	466-2-3	450	25 + 28 m	31.4	28.4	50	After 25 min. a thin (<5 μm) white layer over 5% of surface. After 53 min. sample badly corroded (Fig. 6). About 50% of white phase is dense (as in Fig. 10) and 50% porous (Fig. 9).
9	458-2-4	550	20 + 28 m	31.0	28.6	50	After 20 min. thin (<5 μm) white layer over 75% of surface. After 48 min. white phase over entire surface - about 50% porous. Thin (10 μm) layer of grey phase between white and oxide (similar to Fig. 8).
10	466-2-4	550	20 + 28 m	30.4	28.3	50	After 20 min. thin (<5 μm) white layer over 75% of surface. After 48 min. porous white phase over entire surface (similar to Fig. 9).
11	257	450	45 m	NR	NR	NR	Massive white layer formed (similar to Fig. 7), also thin white layer which showed a laminated structure (Fig. 11).
12**	458-3-2	550	20 m	32.4	NR	20	A thin layer identified as U_3Si_2 observed between U_3Si and USi_2 (Table 4).

* In each case described in this table, an adherent black layer was present on the outside surface. This layer was identified as UO_2 on sample No. 5 (Table 4).

** Oxidized in pure oxygen. NR - Not Recorded.

TABLE 4

MICROPROBE EXAMINATION OF SAMPLES OXIDIZED IN AIR[17,18]

Sample No.	Layer	wt% Si*	wt% U*	Probable Phase
5 (Figs.7 & 8)	Massive white	16.3	-	βUSi_2
	Thin white	15.5		βUSi_2
	Grey	$\approx$3.0	76.9	-
	Outer black	-	87	UO_2
6 (Fig. 9)	Porous white	14.7**	-	βUSi_2
	Solid white	16.1	-	βUSi_2
11 (Fig. 11)	Massive white	18.9	-	αUSi_2
	Thin white	18.7	-	αUSi_2
12+ (Similar to Fig. 18)	Thick white	18.95	-	αUSi_2
	Intermediate	7.60	-	U_3Si_2

* Accuracy ±1%

** Probably low because of porosity

\- Not measured

\+ Oxidized in oxygen

TABLE 5

CHEMICAL DATA ON CORROSION POWDER SAMPLES

Sample No.	Oxidized in	Temperature (°C)	Chemical Analyses			
			O_2 (wt%)	Si (wt%)	U (wt%)	N_2 (ppm)
5	Air	350	15.6*	ND	ND	540
6	Air	350	13.7*	3.2	77.5	ND
9	Air	550	16.4	ND	ND	120
13	Steam	550	16.1	3.1	78.9	ND

* Average of two values - duplicate samples showed variations of ± 2 wt% (No. 6) and ± 1 wt% (No. 5). Other results are for a single sample.

ND - Not done.

TABLE 6

SUMMARY OF RESULTS OF HYDRIDING RUNS ON U_3Si SAMPLES

Sample No.	CRNL Reference No.	Temp. (°C)	Time (hours)	Pressure (Torr)		% Weight Change	Remarks
				Start	Finish		
14	458-1-5	240	2.0	9.80	9.80	Nil	After the high pressure run specimen was light straw color, some of the uranium near the surfaces was partially hydrided and some entirely hydrided (Figure 12). After subsequent oxidation the U_3Si around all of the hydrided uranium particles exhibited a darkened phase (Figure 13).
		200	2.0	9.80	9.80	Nil	
		225	4.0	103.20	100.30	NR	
15	466-1-5	240	2.0	9.80	9.80	Nil	Specimen was a light straw color; no metallographic evidence of hydriding of U_3Si matrix or U_3Si_2 particles.
		200	2.0	9.80	9.80	Nil	
		225	4.1	101.00	101.00	Nil	
16	458-1-2	350	2.0	9.80	9.80	Nil	Specimen was light straw color; no metallographic evidence of hydriding of U or U_3Si matrix.
17	466-1-2	350	2.0	9.80	9.80	Nil	As for No. 15.
18	458-1-3	500	3.5	9.80	9.80	Nil	As for No. 16.
19	466-1-3	500	3.5	9.80	9.80	Nil	As for No. 15.
20	458-3-4	460	4.0	128.4	125.6	<0.001	Specimen barely tarnished; some of the uranium particles touching the outer surface had been partially corroded away probably due to hydride attack. No darkening of U_3Si.

NR - Not Recorded.

TABLE 7 SUMMARY OF PHASE IDENTIFICATION ON SPECIMENS TESTED IN HIGH TEMPERATURE WATER OR STEAM

Sample No.	CRNL Reference Specimen No. (Si - wt%)	Coolant and Exposure Time	Metallographic Results+	Microprobe (wt%) Si	Microprobe (wt%) U	Probable Phase
21	5006 (3.65)	320°C water 3 h	One area which was incompletely deltized corroded badly. Microstructure after corrosion showed			
			a) darkening of U_3Si around U_3Si_2 and U particles; believed to be hydriding (Fig. 14)	Same as U_3Si	Same as U_3Si	U_3Si(H)
			b) badly cracked U_3Si_2 particles	7.3	-	U_3Si_2
22	M-183 (4.0)	350°C steam 5 h	a) intermittent white layer on OD which did not polarize (similar to Fig. 15)	15.90	-	βUSi_2
			b) U_3Si_2 particles in the matrix near white layer	7.3	-	U_3Si_2
23	M-184 (4.0)	450°C steam 1 h	a) U_3Si_2 particles in the matrix	7.6	-	U_3Si_2
			b) An intermittent white layer on OD which did not polarize (Fig. 15). Darkening of U_3Si around particles identified as U_3Si_2 (Fig. 16).	15.40	-	βUSi_2
24	M-90 (4.0)	510°C steam 0.2 h	Possible hydriding around U_3Si_2 particles and at U_3Si grain boundaries (Fig. 17)			
25	M-64 (4.0)	550°C steam 0.2 h	a) white polycrystalline layer on OD (Fig. 18)	16.04	-	βUSi_2
			b) thin layer of U_3Si_2 observed between U_3Si and white layer (Figs. 18 & 19)	7.29	-	U_3Si_2
			c) U_3Si_2 particles observed in U_3Si matrix and across the layer of U_3Si_2 (Fig. 19)	7.3	-	U_3Si_2
			d) U_3Si_2 particles in white layer (Fig. 19)	7.15	-	U_3Si_2
			e) white layer of βUSi_2 stained dark by Murakami's etch (Fig. 19)			
26	M-185 (4.0)	550°C steam 0.2 h	a) badly cracked white layer exhibiting a laminated structure under polarized light	15.62	-	βUSi_2
			b) thin layer between U_3Si and outer white layer - probably U_3Si_2			
			d) U_3Si_2 particles in matrix near βUSi_2 layer	7.2	-	U_3Si_2
27	S - 1* (4.0)	620°C steam ≈4 h	a) light tan phase surrounded by a white phase observed in the corrosion product (Figs. 20 & 21)	≈18.3(tan) 26.5(white)	- -	αUSi_2 USi_3
			b) porous tan phase (adjacent to U_3Si) which contained many particles (Fig. 22)	19.5	-	αUSi_2
			c) particles in the porous tan phase	7.3	-	U_3Si_2
			d) a solid tan phase (adjacent to porous tan phase) which contained few U_3Si_2 particles (Fig. 22)	19.0	-	αUSi_2
			e) breakdown of U_3Si_2 particles into a tan colored phase in advance of the corrosion front	-	-	-
			f) unidentified white filament phase in some U_3Si_2 particles (Fig. 23); believed to be USi_3	-	-	-
28	M-59 (4.0)	295°C water 115 h	white phase (<10 μm thick) at oxide/metal interface	22 ± 2	80	αUSi_2
29	M-35 (4.50)	300°C water 4.5 h	white phase (4 μm thick) on <<5% of surface area	14.6	-	βUSi_2
30	M-21* (3.90)	300°C water 2340 h	Darkening of U_3Si observed around some U_3Si_2 particles; white needle-like phase (believed to be USi_3) seen in U_3Si & U_3Si_2 . Thin intermittent white layer on the surface - could be αUSi_2 (see No. 28).	-	-	-

- not analyzed

+ in each case a layer of oxide was formed on the outside surface of the sample in addition to the white sub-layers described in the table.

* a miniature element with a small defect in the sheath. All other samples bare.

Additional copies of this document
may be obtained from
Scientific Document Distribution Office
Atomic Energy of Canada Limited
Chalk River, Ontario, Canada

Price - $1.00 per copy

3090-71